Reversible Energy Absorption of Elasto-plastic Auxetic, Hexagonal, and AuxHex Structures Fabricated by FDM 4D Printing

To cite this article before publication: N. Namvar *et al* 2022 *Smart Mater. Struct.* in press https://doi.org/10.1088/1361-665X/ac6291

Reversible Energy Absorption of Elasto-plastic Auxetic, Hexagonal, and AuxHex Structures Fabricated by FDM 4D Printing

N. Namvar[1], A. Zolfagharian[2], F. Vakili-Tahami[1] and M. Bodaghi[3,*]

[1]*Department of Mechanical Engineering, University of Tabriz, Tabriz, Iran*

[2]*School of Engineering, Deakin University, Geelong, Victoria 3216 Australia*

[3]*Department of Engineering, School of Science and Technology, Nottingham Trent University, Nottingham NG11 8NS, UK*

(*Corresponding author: mahdi.bodaghi@ntu.ac.uk)

Abstract

The present study aims at introducing reconfigurable mechanical metamaterials by utilising four-dimensional (4D) printing process for recoverable energy dissipation and absorption applications with shape memory effects. The architected mechanical metamaterials are designed as a repeating arrangement of re-entrant auxetic, hexagonal, and AuxHex unit-cells and manufactured using 3D printing fused deposition modelling process. The AuxHex cellular structure is composed of auxetic re-entrant and hexagonal components. Architected cellular metamaterials are developed based on a comprehension of the elasto-plastic features of shape memory polylactic acid materials and cold programming deduced from theory and experiments. Computational models based on ABAQUS/Standard are used to simulate the mechanical properties of the 4D-printed mechanical metamaterials under quasi-static uniaxial compression loading, and the results are validated by experimental data. Research trials show that metamaterial with re-entrant auxetic unit-cells has better energy absorption capability compared to the other structures studied in this paper, mainly because of the unique deformation mechanisms of unit-cells. It is shown that mechanical metamaterials with elasto-plastic behaviors exhibit mechanical hysteresis and energy dissipation when undergoing a loading-unloading cycle. It is experimentally revealed that the residual plastic strain and dissipation processes induced by cold programming are completely reversible through simple heating. The results and concepts presented in this work can potentially be useful towards 4D printing reconfigurable cellular structures for reversible energy absorption and dissipation engineering applications.

1. Introduction

Mechanical meta-materials are engineered materials that are rationally designed to achieve remarkable and unusual mechanical behaviors that may not be found in natural materials [1, 2]. Some examples of these unconventional features are ultrahigh stiffness [3], zero shear modulus [4], zero/negative Poisson's ratio [5], negative stiffness [6], and multi-stability [7-9]. These unique mechanical properties result from their special geometry of repeating unit-cells rather than their constituents [10].

Energy-absorbing structures are widely observed in nature. For instance, bones, hooves, tusks, woods, horns, teeth, and antlers are some of the remarkable biological energy absorbers in nature [11-13]. Mechanical metamaterials and bio-inspired architected lattice materials have been widely employed for various energy absorption and dissipation engineering applications, such as improving vehicles and airplanes crashworthiness, protection against industrial accidents, highway safety, packaging of sensitive goods, and personal safety [14, 15]. In compression, these architected structures absorb a considerable amount of energy without generating high stresses because they can undergo significant compressive strains at roughly a certain stress level. Energy absorption principles in cellular structures may be defined as the ability to convert the input kinetic energy of an impact into other sorts of energy via elastic or plastic deformation, mechanical instabilities, and fracture [16-18]. Energy absorption due to plastic deformation has been the most commonly used mechanism for absorbing energy in ductile materials such as polymers and metals and has the widest practical applications [16, 18]. Recently, Tan et al. [18] investigated a reusable metal-material, stainless steel, that can dissipate energy through plastic deformation and inelastic instability. In their study, the structure's repeatability was examined through cyclic compression and improved by executing an annealing treatment. The results revealed that the proposed reusable metamaterial is repeatable, but increasing the dimensions

reduces the repeatability of the structure. However, these types of energy absorbers have one major disadvantage: failure followed by fracture during several cyclic loading-unloading tests. Shape memory alloys (SMAs) like nickel-titanium (*NiTi*) are advanced materials with unique superelastic and shape memory effects (SMEs) properties that have been developed and used to introduce reversible energy absorbers [19, 20]. The mechanism for energy absorption in SMAs involves the recoverable phase transformation between austenite and martensite.

In the last few decades, the emergence of 3D printing or additive manufacturing technologies has made it possible to manufacture advanced mechanical metamaterials and architected periodic cellular cores with significant complexity for elastic and elasto-plastic deformation [21]. As an example, Bates et al. [22] evaluated energy absorption ability of a honeycomb structure made of thermoplastic polyurethanes (TPUs) and fabricated by fused filament fabrication (FFF) technology. Habib et al. [23] carried out experimental, theoretical, and numerical analyses to investigate the energy absorption capability and compressive fracture properties of 3D printed traditional honeycomb under in-plane uniaxial loading with different wall thicknesses. They have demonstrated that the plastic deformation mechanisms of regular hexagonal cellular structures are different in two perpendicular in-plane directions, X1 and X2. Mirzaali et al. [24] fabricated multi-material lattice structures by using advanced multi-material additive manufacturing methods in order to independently tailor the elastic properties and Poisson's ratio. Taheri Andani et al. [25] used selective laser melting (SLM) technology to manufacture dense and porous NiTi shape memory alloys. It was observed that the NiTi structures have good shape-memory behavior and can be considered as promising materials for lightweight industrial components and energy absorbers. Yazdani Sarvestani et al. [26] studied the out-of-plane and in-plane mechanical properties and energy absorption capability of lightweight sandwich structures with various cellular cells manufactured by the fused deposition modeling (FDM) 3D printing technique. It was seen that the auxetic sandwich panel exhibited better ability for energy absorption applications than the rectangular and hexagonal sandwich panels. Hedayati et al. [27] presented experimental, analytical, and numerical analyses to calculate the yield strength and elastic modulus of 3D-printed Polylactic acid (PLA) structures based on the cube- and diamond-shaped unit-cells manufactured by FDM process. Al-Saedi et al. [28] carried out quasi-static uniaxial compression loading to study the mechanical properties and energy absorption behavior of functionally graded cellular structures made of Al-12Si aluminium alloy and fabricated using SLM technology. Yang et al. [29] proposed some novel self-locking energy absorber models with various shapes fabricated with hard materials like stainless steel and soft photopolymer resin to improve the performance of self-locked structures. Alomarah et al. [30] experimentally and numerically investigated the compressive behavior of re–entrant chiral auxetic structure (RCA) and compared it with three common mechanical lattice structures (tetrachiral, anti–tetrachiral, and re–entrant) made of polyamide12 (PA12) and produced by the Multi Jet Fusion (MJF) process. The results revealed that the RCA structure provided better energy absorption properties than other auxetic honeycombs. Xu et al. [31] performed uniaxial compression loading to investigate the energy absorption capability and in-plane mechanical performance of a novel hybrid structure of combining regular hexagonal and auxetic unit-cells made of nylon material and manufactured by utilizing selective laser sintering (SLS) process. The results demonstrated that the novel architected mechanical metamaterial possessed superior energy absorption performance and Young's modulus compared to the regular hexagonal lattice structure. By combining the structural design and advanced multi-material additive manufacturing processes, Zhao et al. [32] achieved the soft architected lattice metamaterials with thermally controllable auxetics and thermally tunable deformation modes. With the combination of traditional 3D printing procedures and smart materials, the 3D printed objects can change their shapes or properties over time in response to various external stimuli [33, 34]. Therefore, the integration of 3D printing techniques with time as the fourth dimension led to an innovation in printing technology known as 4D printing. For instance, Li et al. [35] proposed 4D printed shape memory PLA occlusion devices with remote controllability for interventional therapy of atrial septal defect. Based on FDM 4D printing technology, Bodaghi et al. [14] explored dual-material auxetic lattice structures with several combinations of hard and soft components for reversible energy absorption engineering applications. Through the experimental tests and numerical analyses, they revealed that their proposed meta-structures could be considered as potential candidates for energy-absorbing applications with a high ability to absorb energy and generate a range of non-linear stiffness. Liu et al. [36] proposed a reversible zero-Poisson's ratio lattice structure with vibration isolation, adjustable mechanical performance, and programmable shapes capability. Through a compression process at various temperatures, the mechanical behaviors of the structure were investigated. Dong et al. [37] carried out uniaxial quasi-static compression loading on metallic re-entrant lattice structures to evaluate and explore the effect of the strut thickness on the deformation mode and negative Poisson's ratio effect on the crushing stress. Two other research works [38, 39] have also been conducted on the study of reversible mechanical metamaterial with impact protection capabilities by 4D printing techniques. It can be seen from above literatures that there are no comprehensive studies on the energy absorption capability and mechanical properties of recoverable cellular structures with negative Poisson's ratio (auxetic), zero Poisson's ratio

(AuxHex), and positive Poisson's ratio (hexagonal) together fabricated by 4D printing method. Furthermore, the open literature does not provide any criteria for judging which structure has a better energy absorption capability.

The present study aims to evaluate and investigate mechanical metamaterials architected with positive, zero and negative Poisson's ratios created using 4D printing method for recoverable energy absorption and dissipation applications. Filament-based FDM, the most commonly used additive manufacturing technique, is implemented to fabricate mechanical lattice structures with re-entrant auxetic, hexagonal, and AuxHex unit-cells from shape memory PLA. It is found that 4D-printed mechanical metamaterials with elasto-plastic features are potentially desirable in dissipating energy due mainly to the mechanical hysteresis phenomena through the plastic deformation mechanism. Finite element method (FEM) is performed by using the commercial software ABAQUS to replicate experimental results on mechanical loading-unloading conditions. It is shown that the presented numerical simulations are successfully able to replicate the non-linear plastic plateau regime, energy absorption capacity, unloading path, and deformation mode observed in the experiments. The results and concepts presented in this study are expected to pave the way for promising exploration of the potential of 4D printed mechanical metamaterials as effective and smart devices for reversible energy absorption and dissipation engineering applications.

2. Conceptual design

2.1. Cold programming

PLA is a thermoplastic shape memory polymer (SMP) with good shape memory behavior that can perfectly recover its initial shape after being fixed into a temporary shape through mechanical deformation via a cold/hot programming method. This shape programming is determined by the temperature zone in which the programming process is carried out. In the case of hot programming for the SMP materials, the structure is initially heated above T_g and loaded mechanically. Next, it is cooled down below T_g while maintaining the deformation load. It is then unloaded. Hereafter, the sample is heated up above T_g to recover its original shape. In many SMP-based energy absorber structures such as car bumpers, hot programming for a shape recovery is not applicable. The structure indeed experiences a cold programming via loading at ambient temperature. In the present work, the cold programming technique is used to program the PLA-based mechanical metamaterials at room temperature, which is below their glassy transition temperature, T_g. This cold programming method and recovery process for dual SME are shown schematically in Fig. 1. In this case, the PLA material is first plastically deformed beyond its yield point at a temperature lower than its T_g, and then unloaded to a temporary deformed shape (steps 1 and 2), see Fig. 1. After programming, the polymer is heated up above its T_g to recover its initial permanent shape (step 3). The mechanically induced plastic strain is potentially recoverable, as shown in Fig. 1. Lastly, the material is cooled down to room temperature (step 4).

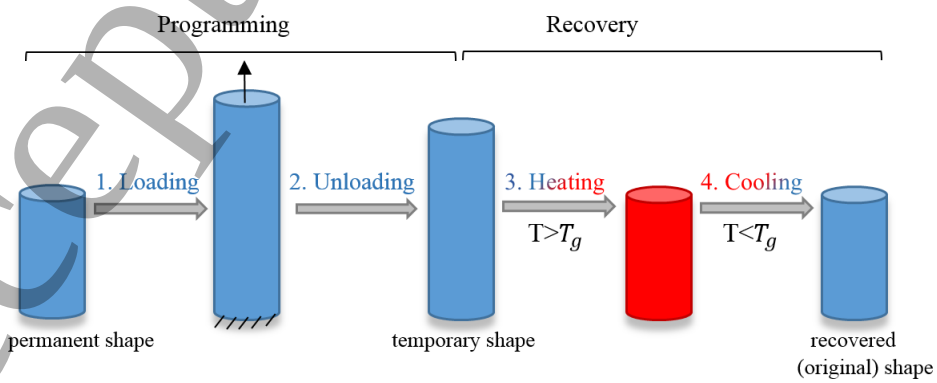

Fig. 1. Schematic diagram of cold programming for SME.

2.2. FDM 3D printing

FDM technology, as one well-known additive manufacturing technique, is employed to manufacture lattice-based structures. FDM 3D printer (3DGence Double P255, Poland) is fed by Polylactic Acid (PLA) filaments (Recreus Inc., Elda, Spain) with a glassy transition temperature of 55℃ and a diameter of 1.75 *mm*. In the FDM process, 3D objects are fabricated from computer-aided design (CAD) models by deposition of a feedstock material in a layer-by-layer technique on a print bed. Before printing, the CAD model of the structures is created by Solidworks software and then converted to Stereolithography (STL) format for the slicing process. The Simplify3D slicing software is used to adjust the STL print settings. Printing parameters such as infill density, printing speed, and layer height are set to 100%, 10 *mm/s*, and 0.2 *mm*, respectively. For the current additive manufactured specimens, the raster angle is set at 0°, which means the tool paths are along the length direction. After slicing, STL files are converted into g-code files and then imported into the FDM 3D printer device to control and command the printing process parameters.

2.3. Material behaviors

In order to explore mechanical properties of the base material (PLA), tensile test samples are 3D printed via FDM according to ASTM standards D638 in a dog-bone shape (Type IV, 2 *mm* thickness) [40]. In this study, four samples of parent material and each structure are examined to obtain clarity of accuracy for the examination results, and the arithmetic mean of all these values is provided as an average value for each set of experiments. It is worthwhile to note that the temperatures of the build platform and nozzle extrusion are set at 60 and 195℃, respectively.

Uniaxial tensile tests are conducted on 3D printed dog-bone samples using the Shimadzu AGS-X 50 kN (Kyoto, Kyoto Prefecture, Japan). All the experimental tests are carried out at a constant crosshead speed of 1 *mm/min* at room temperature, using a load cell of 5 *kN*. It must be noted that all these experiments are performed in a quasi-static manner with a very low strain rate (0.083% s^{-1}) to ensure that there is no viscosity dependency [41].

The tensile stress-strain response of PLA is shown in Fig. 2c. ΔL and F represent displacement and force while L_0 and A_0 refer to length and initial cross-sectional area, respectively. The stress-strain curves of all uniaxial tension samples are considered due to an acceptable consistency. All four samples of PLA dog-bones exhibited similar diagrams with a Young's modulus of 1.4 *GPa* according to the initial linear elastic region, see the red dashed line in Fig. 2c. Poisson's ratio value of the 3D-printed PLA is also calculated as 0.32. As shown in Fig. 2c, plasticity begins at 2.1% strain and PLA reaches a maximum stress of 46.94 *MPa* before break-down. The material behavior can be classified as elasto-plastic due to the change in the slope of the stress-strain curve and residual deformation after unloading before break-down.

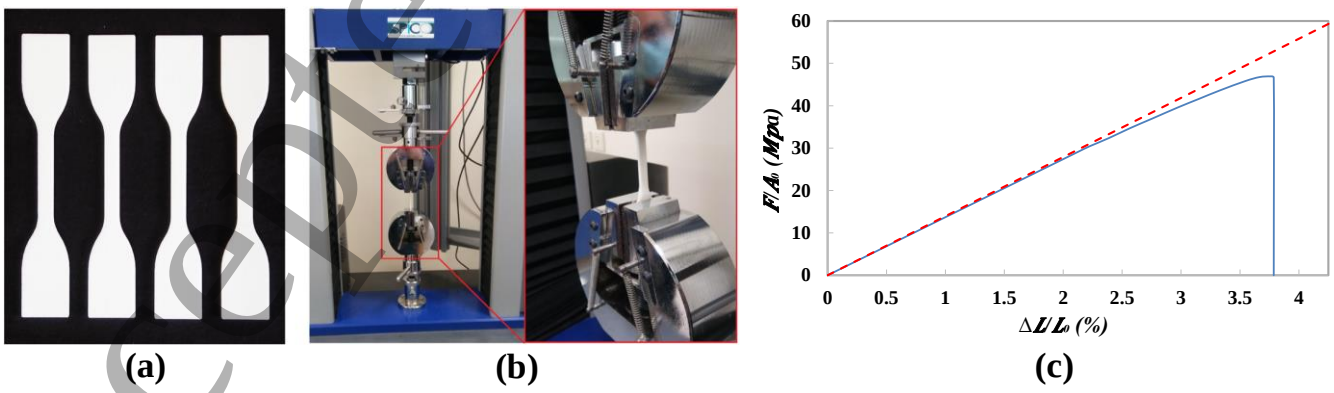

Fig. 2. (a) Four tensile test specimens according to ASTM D638 (Type IV), (b) universal tensile test machine, (c) strain-stress curve of 3D-printed PLA (dashed red line shows the slope of the linear elastic domain).

2.4. Structural Design

Meta-structures geometrical parameters have a significant role in the structural performance. The impact of geometrical design parameters on energy absorption capability and auxeticity of architected cellular metamaterials has been investigated in several research studies [30, 42-47]. Yang et al. [45] found that the absolute value of the Poisson's ratio of the re-entrant lattice metamaterial becomes greater with increasing re-entrant angle and decreasing horizontal-to-inclined strut length ratio. The maximum auxeticity was found for mechanical metamaterials constructed of slender struts, with a horizontal to oblique strut length ratio of 2 and a re-entrant angle of 60°–70° [45-47]. Furthermore, Wang et al. [47] observed that the increase in cell-wall thickness of the re-entrant lattice structure leads to an increase in the density and Young's modulus while the auxetic effect declines gradually. Also, it was discovered that with an increase in relative density, capability for energy absorption increases [42, 43]. Therefore, thickening of the cell-wall of the re-entrant cellular structure leads to an increase not only in relative density, but also in the capability for energy absorption. The aim of this study is to introduce mechanical lattice structures with high energy absorption capabilities. As illustrated in Fig. 3a, for the re-entrant lattice structure, the strut thickness of 0.75 *mm*, the horizontal to inclined strut length ratio of 2 and the re-entrant angle of 60° are simulated by considering the minimum possible resolution of the FDM 3D printing technique.

Three architected mechanical metamaterials are created in the following forms: re-entrant auxetic, hexagonal, and AuxHex. These lattice structures are designed with the same overall dimensions and thickness as depicted in Figs. 3a-f. The AuxHex lattice structure contains two different types of cells: hexagonal and auxetic re-entrant components. Based on the concept of periodicity, the unit-cells of each type are arrayed in the plane to form the initial two-dimensional (2D) construction, as shown in Figs. 3d-f. A 3D CAD model of the re-entrant auxetic, hexagonal, and AuxHex cellular structures is illustrated in Figs. 4a-c, respectively. Architected mechanical metamaterials are prepared in CAD format by Solidworks software. A typical image of the printed specimens is presented in Fig. 5. The energy absorption capacity of the proposed cellular mechanical metamaterials is studied in this paper. It is worth mentioning that the indenter employed in the compression process, assumed as a rigid body, is a combination of a rectangle and a semi-circle.

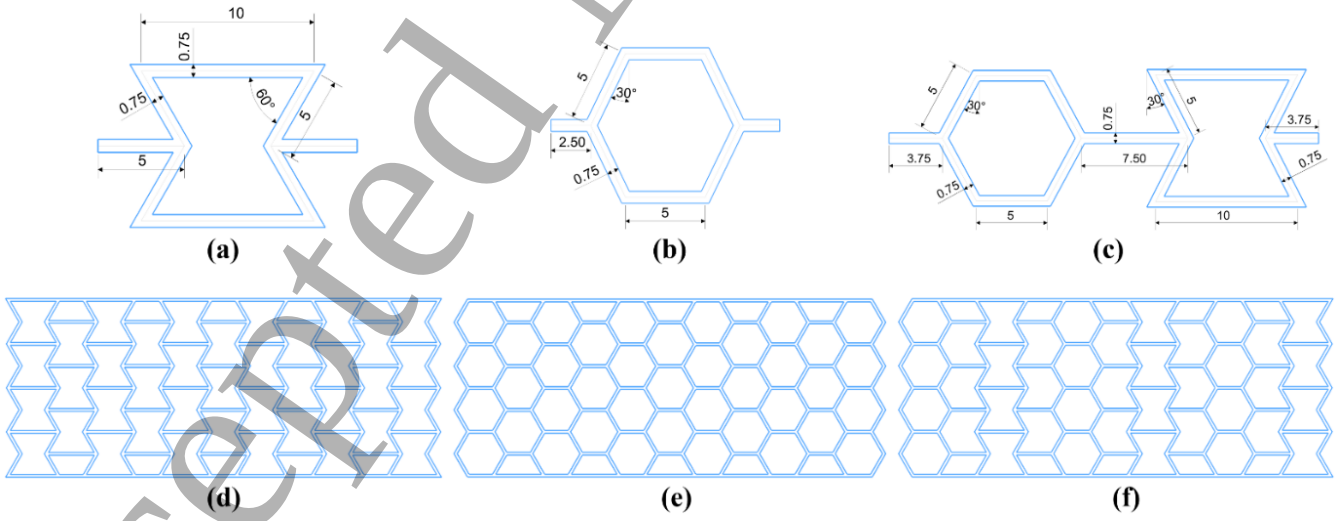

Fig. 3. Single unit-cell geometry and lattice schematic of different lattice metamaterials studied in this research: (a) re-entrant auxetic, (b) hexagonal, (c) AuxHex.

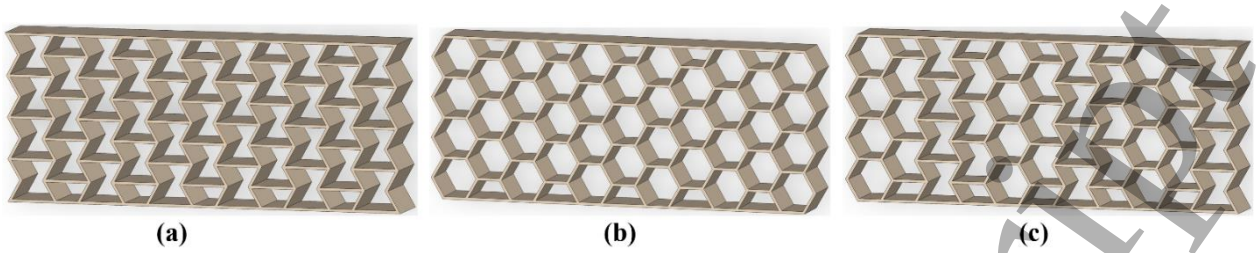

Fig. 4. 3D CAD models of architected cellular metamaterials: (a) re-entrant auxetic, (b) hexagonal, (c) AuxHex.

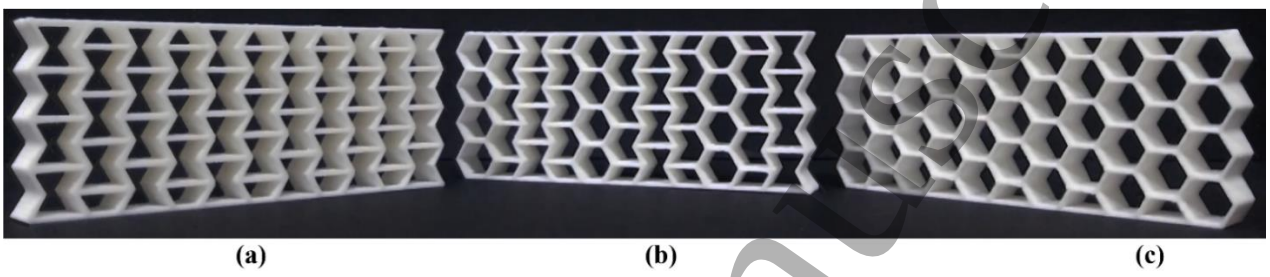

Fig. 5. 3D printed mechanical metamaterials for compression tests: (a) re-entrant auxetic structure, (b) AuxHex structure, (c) hexagonal structure.

3. Results and Discussion

Mechanical behaviors and energy absorption capacity of 4D- printed mechanical metamaterials with three different cell topologies are investigated experimentally and numerically in this section. The 3D-printed indenter that compresses the energy absorbing lattices is attached to the top of the testing machine compression plate and quasi-static compression loading with constant crosshead speed of 1 *mm/min* at ambient temperature ~ 23℃ is applied to the architected lattice metamaterials. The PLA material is expected to exhibit elasto-plastic behavior due to the very low strain rate (0.03% s^{-1}) [41]. Force-displacement curves of all three architected cellular metamaterials are illustrated in Fig. 6. The compression stroke is performed on each sample up to a 15 *mm* axial displacement, which plastically deforms the lattices. Fig. 6 shows that the hexagonal, auxetic re-entrant, and AuxHex meta-structures reach a maximum force of 564, 954, and 652 *N*, respectively. After unloading, a central displacement of 11.95, 11.18, and 11.61 *mm* remains via plastic deformation, respectively, for hexagonal, auxetic re-entrant, and AuxHex meta-structures, as shown in Fig. 6. Finally, Fig. 6 shows that these mechanical metamaterials can be potentially used as energy absorbers for various applications.

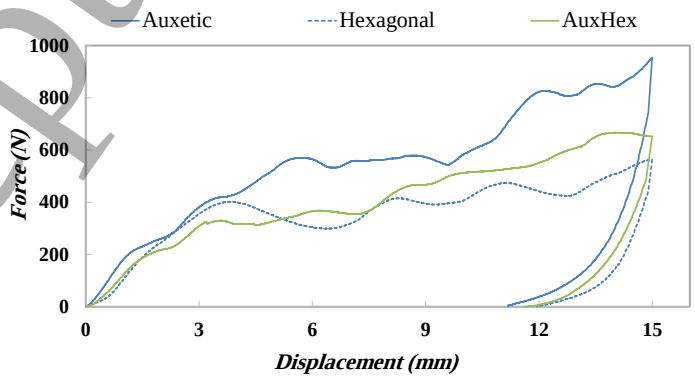

Fig. 6. Experimental force-displacement curves of mechanical metamaterials with three different cell topologies under a quasi-static compressive loading-unloading cycle.

To replicate the mechanical loading-unloading responses of 3D-printed lattice structures with elasto-plastic features, FEM is carried out by using the commercial ABAQUS/Standard solver. A series of FEM models with different geometries is created with the geometrical size mentioned in Figs. 3a-c. A triangular element with a structured 3-node linear is employed in all FEM models to mesh the lattice models. The FEM mesh is generated on the models as illustrated in Figs. 7a-c. In all models, the accuracy of the FEM analysis results can be ensured by using an average mesh size of 0.7 *mm*. The total number of elements after convergence for hexagonal, auxetic re-entrant, and AuxHex models are 2394, 2948, and 2644 respectively. It is worthwhile to mention that the base material properties are needed as an input for the FEM analysis according to the tensile test results mentioned in Fig. 2c. In the simulation, energy-absorbing lattices are placed between the bottom rigid plate and the top indenter. Surface-to-surface contacts are used to simulate the interaction between the cell walls of the structure with themselves as well as the rigid indenter and the model during compression. In addition, the bottom plate is totally constrained, whereas the top indenter is only free to move vertically at a constant velocity and the mechanical lattice structures are completely free without any constraints. It must be noted that, simulating the heating-cooling operation in PLA material requires employing complex constitutive equations [38, 48] which is beyond the purpose of this research and is suggested to be investigated in future studies.

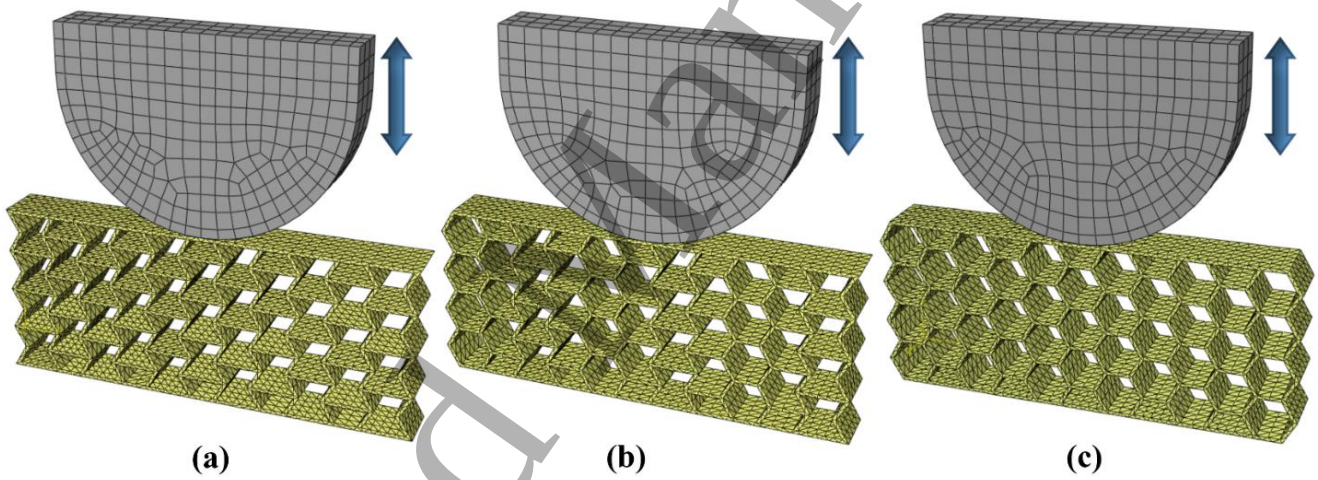

Fig. 7. The lattice metamaterials with generated mesh: (a) re-entrant auxetic structure, (b) AuxHex structure, (c) hexagonal structure.

Experimental and FEM results of three different energy absorbing lattices during loading-unloading cycles are presented in Figs. 8–10, respectively, for re-entrant auxetic, hexagonal, and AuxHex meta-structures. To explore the shape recovery properties of lattice-based energy absorbers after loading and unloading at ambient temperature (23℃), all three mechanical metamaterials are heated up to 80℃, which is above their T_g, and then cooled down to the ambient temperature. Parts (a)-(c) and (e)-(g) of Figs. 8, 9 and 10, show configurations of the architected lattice metamaterials during ambient-temperature loading-unloading derived from experimental tests and FEM simulations, respectively, whereas part (d) displays the configuration of the samples after being heated to 80℃ and then cooled to ambient temperature, 23℃. The force-displacement responses of specimens from the numerical simulation and experiments are also compared in part (h). Part (i) of Figs. 8, 9, and 10 also illustrates the absorbed energy and dissipated energy through the plastic deformation mechanism and mechanical instabilities undergoing a loading-unloading cycle. For the sake of calculation, the energy dissipation is the area within the load-unload curve vs. displacement (graphically described in Fig.8 (i)) and the energy absorption is the area beneath the unload-displacement curve. Finally, to show the main difference between solid structures and lattice structures, the mechanical behavior of a solid structure with the same total volume, material and loading conditions of the re-entrant auxetics is investigated. Its force-displacement is shown in Fig. 8 (h) with a dashed line.

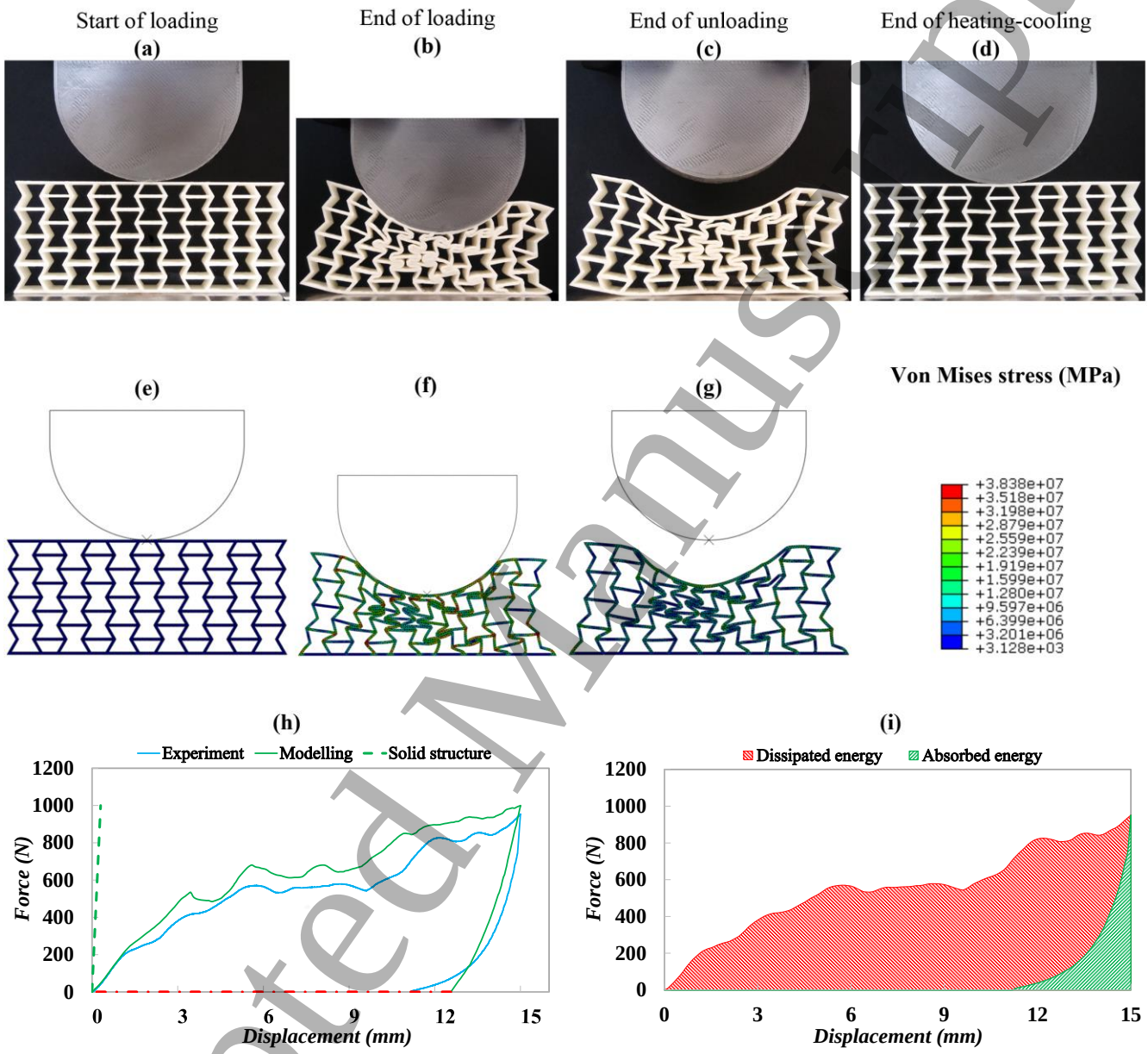

Fig. 8. Re-entrant auxetic mechanical metamaterial: (a)-(g) experimental and FEM simulated compressive deformations, (h) comparison of experimental measured and numerical force-displacement response undergoing a loading-unloading cycle and shape-memory recovery (the red dash-dotted line represents strain recovery by simply heating), (i) absorbed and dissipated energies.

The initial conclusion that can be drawn from Figs. 8–10 is the fact that numerical simulation carried out by using the commercial software ABAQUS as a straightforward tool is capable of accurately replicating the configuration and force-displacement responses of different mechanical lattice structures. Local bending and buckling are observed in the re-entrant lattice structure beam by applying a compressive axial loading, as shown in Fig. 8. It is observed that the auxetic effect of the structure leads to an initial hardening behavior during elastic deformation of the auxetic structure. As shown in Fig. 8h, the force of both experiments and FEM simulation increases linearly with axial displacement at the beginning of the mechanical loading. After the linear elastic regime, the structure enters the plateau

regime, and the force slope begins to decrease slowly. This regime continues till the final densification regime starts, see Fig. 8h. As illustrated in Fig. 8b, the auxetic metamaterial shows shrinkage in both transverse and axial directions upon axial compression loading. In fact, with further compression in the vertical direction, the re-entrant lattice metamaterial starts to contract laterally, and the material flows into the impact zone creating a denser structure. As can be seen in Fig. 8h, these auxetic features influence the mechanical performance and a local hardening or densification phenomenon occurs. When the ligaments contact each other at the end of compressive loading, the re-entrant lattice structure tends to harden, as seen in Fig. 8b, f, and h. The peak forces of 954 and 997 *N* are measured by the experiment and numerical solution, respectively, during the compression loading. Experimental and numerical results demonstrated that special geometries of auxetic mechanical metamaterial result in stiffening of the structure in the region of impact, which can potentially be useful for applications with high impact resistance. By comparing the force-displacement of the auxetic structure with the solid structure, the initial peak force of the specimen decreases when using re-entrant topology, which is beneficial to prevent damage or injury. In addition, the auxetic lattice structure displays a long plateau regime than the solid structure which is desirable from an energy absorption perspective. It can be seen from Fig. 8h that the displacement of the solid structure with the same volume, material and loading conditions is much smaller than what is observed in the auxetic cellular structure. Therefore, the cellular structures are desirable since they can experience large deformations under nearly constant plateau force level, and absorb tremendous amounts of energy [15]. The loading and unloading curves clearly do not coincide with each other. That exhibits a mechanical hysteresis under a quasi-static compressive loading-unloading cycle. It is observed that by mechanical unloading, some plastic strains remain in the re-entrant lattice structure, which reveals the energy dissipation due to the plastic deformation mechanism. These structures convert the input energy of a moving body into the kinetic energy in a cycle and dissipate part of it through plastic deformation. The FEM ABAQUS could successfully replicate the residual plastic deformation in the PLA lattice structure as illustrated in Fig. 8c, g, and h. When the deformed re-entrant lattice structure is heated up above its transition temperature under a stress-free condition, it releases all the residual plastic strains and perfectly recovers its initial shape, as depicted in Fig. 8d. Therefore, the proposed lattice structure is a promising metamaterial that can potentially be applied as recoverable energy absorbers. Comparing FEM simulations with the corresponding experimental data in Fig. 8h shows that there are a few differences in the value of response force. The main rationale behind this difference could be associated with the geometrical imperfection in the real 3D printed lattice structures, while FEM simulation is based on an ideal model with perfect geometry. Nevertheless, the reasonably good agreement between the experimental data and present FEM simulation results, demonstrates that the numerical simulation approach used here can accurately replicate the hysteresis area, unloading path, yield stress, plastic deformation growth and configuration of the unit-cells during loading and unloading. As a result, the FEM simulation is found to be remarkably accurate guidance to simulate the behaviors of 4D-printed mechanical metamaterial. It is worth noting that the area under the load-displacement curve characterizes the energy distribution for the lattice structures, as presented in Fig. 8i. As shown in Fig. 8i, an indicator of the energy dissipation due to the plastic deformation is the area enclosed by loading and unloading curves [14, 18, 49]. The computed energy absorption and dissipation for re-entrant lattice structure are 0.8 *J* and 8.23 *J*, respectively. Because of the existence of plastic hardening characteristics in the PLA material, more energy is dissipated than absorbed for this structure. A similar conclusion was drawn from polyurethane-based SMPs in Ref. [14]. Shape fixity and shape recovery rate are two crucial criteria in determining shape memory behavior of PLA materials. Shape recovery rate quantifies the ability of the SMPs to recover their original shape whereas shape fixity measures the ability of specimen to fix the temporary deformation during the programming process. Shape fixity and shape recovery rate for the auxetic cellular structure are 74.53% and 100%, respectively. In the past, the unusual mechanical properties associated with auxeticity has been employed as an exciting paradigm for developments of impact resistant structures with pure elastic and irrecoverable elastic-plastic behaviors. A far better way is to manufacture auxetic lattices from recoverable SMPs. Fig. 8 shows the ability to fabricate auxetic cellular structures from recoverable stimuli-responsive SPMs and offers a wide range of potential applications under low-velocity impacts like sport gears, helmets, segments in car bumpers, lightweight landing gears, etc.

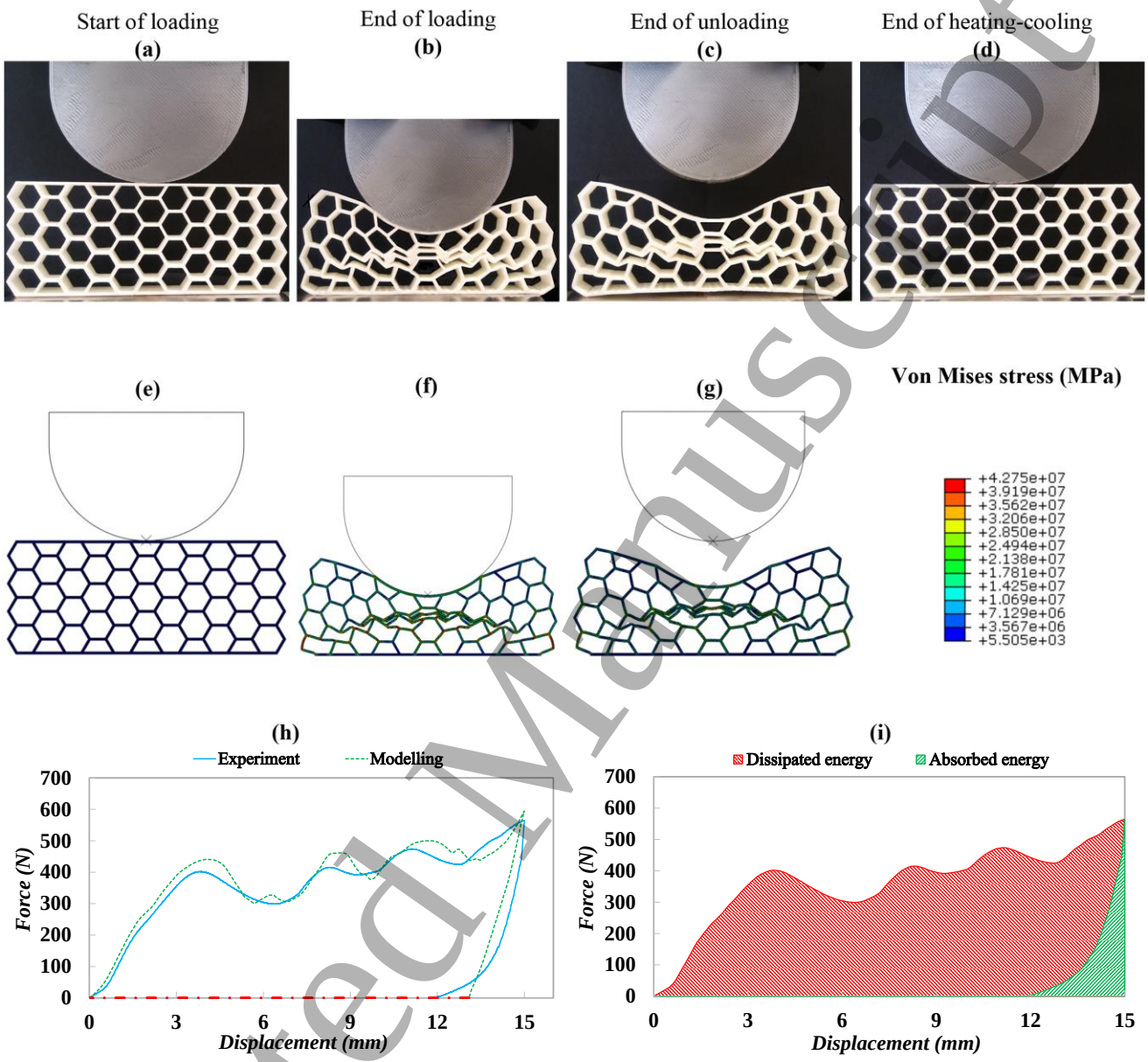

Fig. 9. Hexagonal mechanical metamaterial: (a)-(g) experimental and FEM simulated compressive deformations, (h) comparison of experimental measured and numerical force-displacement response undergoing a loading-unloading cycle and shape-memory recovery (the red dash-dotted line represents strain recovery by simply heating), (i) absorbed and dissipated energies.

The counterparts of Fig. 8 for hexagonal honeycomb and AuxHex structures are presented in Figs. 9 and 10. The preliminary conclusion that can be drawn from Figs. 8 and 9 is that the mechanical responses of architected cellular structures with hexagonal and re-entrant unit-cells are very different. First, an almost linear force-displacement region is observed in Fig. 9h, where the bending occurs in cell walls. Once the hexagonal lattice reaches a critical stress in the walls, the structure starts to collapse and overall snap-through buckling occurs, which suddenly results in softening behavior. When the cell struts start to contact each other, the cell collapse ends and the hexagonal structure tends to harden. Hexagonal honeycomb undergoes successive softening-hardening behavior during mechanical loading step until all collapsed rows touch each other and complete densification occurs. It should be mentioned that such a large oscillation in the force-displacement curve could be due to stress concentration occurring in a certain row and layer-by-layer crushing. As illustrated in Figs. 9b and f, the deformation pattern in both experiments and FEM simulations of the hexagonal honeycomb structure is symmetric. It is seen that the mechanical hysteresis is produced

by removing the load. As can be seen in Fig. 9d, by simply heating the unconstrained hexagonal lattice, the original shape can be fully recovered. The experimental result and the numerical simulation are in good correlation in terms of force-displacement graphs, as shown in Fig. 9h, and both reach approximately similar applied maximum forces during the compression process, which are 564 *N* and 595 *N*, respectively. The computed values for total energy distributed, energy dissipation, and absorption for hexagonal honeycomb are 5.81 *J*, 5.42 *J* and 0.39 *J*, respectively. The results reveal that the energy absorption capability of the metamaterial with hexagonal unit-cells is less than the re-entrant auxetic cellular structure. Shape fixity and shape recovery rate for the hexagonal lattice structure are 79.66% and 100%, respectively.

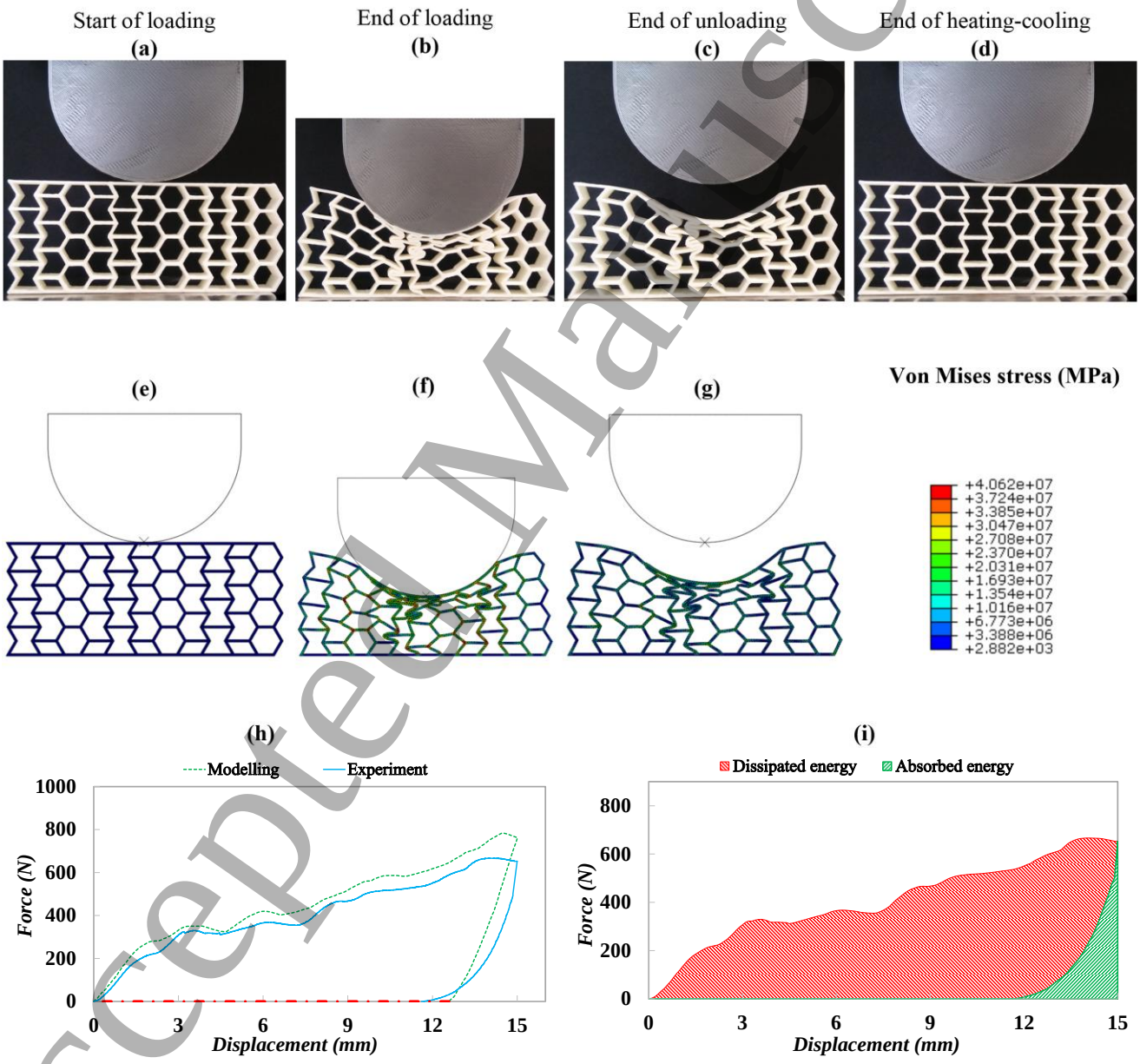

Fig. 10. AuxHex mechanical metamaterial: (a)-(g) experimental and FEM simulated compressive deformations, (h) comparison of experimental measured and numerical force-displacement response undergoing a loading-unloading cycle and shape-memory recovery (the red dash-dotted line represents strain recovery by simply heating), (i) absorbed and dissipated energies.

The mechanical response of the architected cellular structure with AuxHex unit-cells, obtained from experimental tests and numerical simulations, is depicted in Fig. 10. The force first increases linearly with axial displacement, up to a very small displacement of around 1.4 *mm*, as shown in Fig. 10h. It must be noted that after the elastic regime, with a further increase in the axial displacement, the structure enters the plateau region, and the force slope begins to decrease slowly due to the plastic buckling of critical walls. The fluctuations of the plateau regime are attributed to the sequential collapse by buckling of the layers or ligaments. It is worth mentioning that the fluctuation in the plateau regime of the AuxHex lattice structure is much smaller than that observed in the metamaterial with hexagonal unit-cells, which can be attributed to the stable and uniform deformation mechanism and stress distribution of the AuxHex cells. Finally, it can be found from Figs. 10b, f and h that, beyond 10.5*mm* displacement, there is a general hardening trend in force-displacement curve where the collapsed layers touch each other that means the densification phenomenon has occurred. In general, by comparing experimental and numerical results in Fig. 10h, it is found that the present FEM is capable of well replicating the structural behavior with an excellent agreement under such a large deformation. However, there are slight deviations between the experimental and FEM simulated forces due to the manufacturing defects in the cellular metamaterial manufactured by 3D printing, which affect the mechanical performance. The total energy of the AuxeHex lattice structure during the loading-unloading process is computed at 6.62 *J* with energy absorption of 0.53 *J* and energy dissipation of 6.09 *J*. The amounts of the applied maximum forces during the compression loading from the numerical simulation and experiment are 773 *N* and 652 *N*, respectively. It is also observed that when the force is gradually released, the lattice deformation is partially recovered while some plastic strains remain in the cellular mechanical metamaterial and there is a mechanical hysteresis. From the configuration of the AuxHex cellular structure after the heating and cooling cycle depicted in Fig. 10d, it can be found that lattice structure releases all plastic strains and gets back to its original stable shape. It is worth noticing that energy dissipation/absorption performance of AuxHex cellular metamaterial from the quantitative viewpoint is located between those of the re-entrant lattice metamaterial and regular hexagonal honeycomb. These findings support the conclusion that the re-entrant auxetic cellular structure displays a better energy absorption capability than the hexagonal and AuxHex meta-structures. This is directly related to unit-cell shape and different deformation mechanisms during compressive axial loading, which have a significant influence on the mechanical performance of the lattice metamaterials. Shape fixity and shape recovery rate for the AuxHex meta-structure are 77.4% and 100%, respectively.

Conclusion

The energy absorption characteristics and structural mechanical behavior of 4D-printed lattice metamaterials with reversible shape memory properties were investigated in this research. The architected cellular metamaterials were designed as repeating arrangements of re-entrant auxetic, hexagonal, and AuxHex unit-cells and fabricated by FDM 3D printing technology from PLA polymers with a thermally induced shape memory effect. The numerical models were employed using ABAQUS/Standard to simulate the mechanical responses of the 4D-printed mechanical metamaterials under quasi-static compression loading and verified by the experiments. It was found that metamaterial with re-entrant auxetic unit-cells has a higher energy absorption capacity compared to other cell topologies studied in this paper, mainly because of the unique deformation mechanisms of unit-cells. Comparison of experimental and FEM results clearly demonstrated that the simulation approach used here could accurately replicate the yield stress, non-linear plastic plateau regime, unloading path, hysteresis area, and configuration of the unit-cells during loading-unloading. The reversibility of the dissipation processes and residual plastic deformation were revealed experimentally. The results gathered in this work could pave the way for the implementation and development of reversible energy absorption and dissipation devices for shock isolation and protection in multiple impact applications.

References

1. Nicolaou, Z.G. and A.E. Motter, *Mechanical metamaterials with negative compressibility transitions.* Nature materials, 2012. **11**(7): p. 608-613.

2. Mirzaali, M.J., et al., *Non-affinity in multi-material mechanical metamaterials.* Scientific Reports, 2020. **10**(1): p. 11488.
3. Zheng, X., et al., *Ultralight, ultrastiff mechanical metamaterials.* Science, 2014. **344**(6190): p. 1373-1377.
4. Kadic, M., et al., *On the practicability of pentamode mechanical metamaterials.* Applied Physics Letters, 2012. **100**(19): p. 191901.
5. Chen, Y., et al., *Lattice Metamaterials with Mechanically Tunable Poisson's Ratio for Vibration Control.* Physical Review Applied, 2017. **7**(2): p. 024012.
6. Dudek, K., et al., *Negative and positive stiffness in auxetic magneto-mechanical metamaterials.* Proceedings of the Royal Society A: Mathematical, Physical and Engineering Sciences, 2018. **474**(2215): p. 20180003.
7. Haghpanah, B., et al., *Architected Materials: Multistable Shape-Reconfigurable Architected Materials (Adv. Mater. 36/2016).* Advanced Materials, 2016. **28**(36): p. 8065-8065.
8. Rafsanjani, A., A. Akbarzadeh, and D. Pasini, *Metamaterials: Snapping Mechanical Metamaterials under Tension (Adv. Mater. 39/2015).* Advanced Materials, 2015. **27**(39): p. 5930-5930.
9. Che, K., et al., *Three-dimensional-printed multistable mechanical metamaterials with a deterministic deformation sequence.* Journal of Applied Mechanics, 2017. **84**(1).
10. Cui, T.J., D.R. Smith, and R. Liu, *Metamaterials*. 2010: Springer.
11. McKittrick, J., et al., *Energy absorbent natural materials and bioinspired design strategies: a review.* Materials Science and Engineering: C, 2010. **30**(3): p. 331-342.
12. San Ha, N. and G. Lu, *A review of recent research on bio-inspired structures and materials for energy absorption applications.* Composites Part B: Engineering, 2020. **181**: p. 107496.
13. Rahman, H., et al., *Energy absorption and mechanical performance of functionally graded soft–hard lattice structures.* Materials, 2021. **14**(6): p. 1366.
14. Bodaghi, M., et al., *Reversible energy absorbing meta-sandwiches by FDM 4D printing.* International Journal of Mechanical Sciences, 2020. **173**: p. 105451.
15. Lu, G. and T. Yu, *Energy absorption of structures and materials*. 2003: Elsevier.
16. Svensson, E., *Material characterization of 3D-printed energy-absorbent polymers inspired by nature*. 2017.
17. Sun, S., et al., *Snap-back induced hysteresis in an elastic mechanical metamaterial under tension.* Applied Physics Letters, 2019. **115**(9): p. 091901.
18. Tan, X., et al., *Reusable metamaterial via inelastic instability for energy absorption.* International Journal of Mechanical Sciences, 2019. **155**: p. 509-517.
19. Nemat-Nasser, S., et al., *Quasi-Static and Dynamic Buckling of Thin Cylindrical Shape-Memory Shells.* Journal of Applied Mechanics, 2005. **73**(5): p. 825-833.
20. Jiang, D., et al., *Buckling and recovery of NiTi tubes under axial compression.* International Journal of Solids and Structures, 2016. **80**: p. 52-63.
21. Zadpoor, A.A., *Additively manufactured porous metallic biomaterials.* Journal of Materials Chemistry B, 2019. **7**(26): p. 4088-4117.
22. Bates, S.R.G., I.R. Farrow, and R.S. Trask, *3D printed polyurethane honeycombs for repeated tailored energy absorption.* Materials & Design, 2016. **112**: p. 172-183.
23. Habib, F.N., et al., *In-plane energy absorption evaluation of 3D printed polymeric honeycombs.* Virtual and Physical Prototyping, 2017. **12**(2): p. 117-131.
24. Mirzaali, M.J., et al., *Multi-material 3D printed mechanical metamaterials: Rational design of elastic properties through spatial distribution of hard and soft phases.* Applied Physics Letters, 2018. **113**(24): p. 241903.

25. Andani, M.T., et al., *Mechanical and shape memory properties of porous Ni50. 1Ti49. 9 alloys manufactured by selective laser melting.* Journal of the mechanical behavior of biomedical materials, 2017. **68**: p. 224-231.
26. Yazdani Sarvestani, H., et al., *3D printed architected polymeric sandwich panels: Energy absorption and structural performance.* Composite Structures, 2018. **200**: p. 886-909.
27. Hedayati, R., et al., *Semianalytical Geometry-Property Relationships for Some Generalized Classes of Pentamodelike Additively Manufactured Mechanical Metamaterials.* Physical Review Applied, 2019. **11**(3): p. 034057.
28. Al-Saedi, D.S.J., et al., *Mechanical properties and energy absorption capability of functionally graded F2BCC lattice fabricated by SLM.* Materials & Design, 2018. **144**: p. 32-44.
29. Yang, K., et al., *Shape and geometry design for self-locked energy absorption systems.* International Journal of Mechanical Sciences, 2019. **156**: p. 312-328.
30. Alomarah, A., et al., *Compressive properties of 3D printed auxetic structures: experimental and numerical studies.* Virtual and Physical Prototyping, 2020. **15**(1): p. 1-21.
31. Xu, M., et al., *Mechanical properties and energy absorption capability of AuxHex structure under in-plane compression: Theoretical and experimental studies.* International Journal of Mechanical Sciences, 2019. **159**: p. 43-57.
32. Zhao, Z., et al., *Three-Dimensionally Printed Mechanical Metamaterials With Thermally Tunable Auxetic Behavior.* Physical Review Applied, 2019. **11**(4): p. 044074.
33. Truby, R.L., et al., *Soft somatosensitive actuators via embedded 3D printing.* Advanced Materials, 2018. **30**(15): p. 1706383.
34. Lei, D., et al., *A general strategy of 3D printing thermosets for diverse applications.* Materials Horizons, 2019. **6**(2): p. 394-404.
35. Lin, C., et al., *4D-Printed Biodegradable and Remotely Controllable Shape Memory Occlusion Devices.* Advanced Functional Materials, 2019. **29**(51): p. 1906569.
36. Liu, K., et al., *4D printed zero Poisson's ratio metamaterial with switching function of mechanical and vibration isolation performance.* Materials & Design, 2020. **196**: p. 109153.
37. Dong, Z., et al., *Experimental and numerical studies on the compressive mechanical properties of the metallic auxetic reentrant honeycomb.* Materials & Design, 2019. **182**: p. 108036.
38. Bodaghi, M. and W. Liao, *4D printed tunable mechanical metamaterials with shape memory operations.* Smart Materials and Structures, 2019. **28**(4): p. 045019.
39. Yang, C., et al., *4D printing reconfigurable, deployable and mechanically tunable metamaterials.* Materials Horizons, 2019. **6**(6): p. 1244-1250.
40. Properties, A.S.D.o.M. *Standard test method for tensile properties of thin plastic sheeting*. 1995. American Society for Testing and Materials.
41. Guo, X., et al., *Influence of strain rates on the mechanical behaviors of shape memory polymer.* Smart Materials and Structures, 2015. **24**(9): p. 095009.
42. Yuan, S., C.K. Chua, and K. Zhou, *3D-Printed Mechanical Metamaterials with High Energy Absorption.* Advanced Materials Technologies, 2019. **4**(3): p. 1800419.
43. Gibson, L.J., *Cellular solids.* Mrs Bulletin, 2003. **28**(4): p. 270-274.
44. Li, D., et al., *Comparison of Mechanical Properties and Energy Absorption of Sheet-Based and Strut-Based Gyroid Cellular Structures with Graded Densities.* Materials, 2019. **12**(13): p. 2183.
45. Yang, L., et al., *Mechanical properties of 3D re-entrant honeycomb auxetic structures realized via additive manufacturing.* International Journal of Solids and Structures, 2015. **69-70**: p. 475-490.
46. Li, S., et al., *The development of TiNi-based negative Poisson's ratio structure using selective laser melting.* Acta Materialia, 2016. **105**: p. 75-83.
47. Wang, X.-T., X.-W. Li, and L. Ma, *Interlocking assembled 3D auxetic cellular structures.* Materials & Design, 2016. **99**: p. 467-476.

48. Xin, X., et al., *Mechanical Models, Structures, and Applications of Shape-Memory Polymers and Their Composites.* Acta Mechanica Solida Sinica, 2019. **32**(5): p. 535-565.
49. Siddique, S.K., et al., *Nanonetwork Thermosets from Templated Polymerization for Enhanced Energy Dissipation.* Nano letters, 2021. **21**(8): p. 3355-3363.